J Mater Sci (2008) 43:3296–3304
DOI 10.1007/s10853-008-2525-1

Lap joint properties of FSWed dissimilar formed 5052 Al and 6061 Al alloys with different thickness

Chang-Yong Lee · Won-Bae Lee · Jong-Woong Kim · Don-Hyun Choi · Yun-Mo Yeon · Seung-Boo Jung

Received: 17 November 2007 / Accepted: 1 February 2008 / Published online: 5 March 2008

Abstract Lap joint friction stir welding (FSW) between dissimilar 5052-H112 (1 mm) and 6061-T6 (2 mm) Al alloys with different thickness was carried out with various tool rotation speeds and welding speeds according to the fixed location of each material on bottom or top sheet. Interface morphology was characterized by pull-up or pull-down from initial joint line. Amount of vertical material transports increased and thickness of 5052 resultantly lessened with increasing tool rotation and decreasing welding speed, which were the conditions of the weak bond. Higher stress concentration on the interface pull-up region, the penetration of unbonded region into the weld zone and the lessened thickness of 5052 Al part might be the reasons for lower fracture load. Higher fracture load was acquired at the lower tool rotation speed and higher welding speed when a thicker 6061 was fixed at retreating side on top sheet. Interface morphology was the most important factor determining the mechanical strength of lap FSW joints and can be manageable using FSW parameters.

C.-Y. Lee · J.-W. Kim · D.-H. Choi · S.-B. Jung (✉)
School of Advanced Materials Science & Engineering, Sungkyunkwan University, 300 Cheoncheon-dong, Jangan-gu, Suwon 440-746, South Korea
e-mail: sbjung@skku.ac.kr

W.-B. Lee
Joining Research Group, Technical Research Laboratories, POSCO, Geodong-dong, Nam-gu, Pohang 790-895, South Korea

Y.-M. Yeon
Department of Automated System, Suwon Science College, 9-10 Botong-li, Jungnam-myeon, Hwasung, Gyeonggi-do 445-742, South Korea

Introduction

Friction stir welding (FSW) is a solid-state bonding method which was developed by TWI in 1991[1]. Since then, it has attracted attention as a revolutionary welding method which could solve the problems associated with the fusion welded Al alloys, and hence it has been the subject of many studies to apply the method in service applications [2–5].

The process has been mainly used for making butt joints in Al alloys. Recently, FSW has been used in lap joint production that expands the number of applications that could benefit from the technique.

There have been some studies about FSW for lap joint [6, 7]. In lap joint FSW, the movement of materials within the weld is more important than the microstructure, due to the interface present between the sheets and vertical transport of materials about longitudinal axis of the weld. If a vertical motion of material took place outside the pin diameter, the unbonded sheet interface materials could be transported vertically, affecting the strength of the lap weld due to the application of the bending force. However, various interface phenomena and mechanical properties with welding conditions, e.g., tool rotation, welding speed, and fixing location of welded materials, were not clearly examined.

In this study, dissimilar 5052-H112 and 6061-T6 Al alloys were friction stir welded by lap joint type with various tool rotation speeds and welding speeds. Especially, each weld set was divided into cases A and B according to friction stir lap welding construction (details are in the experimental procedure). The morphology of interface, formation of onion ring (related to metal flow), and microstructure were observed and mechanical properties, such as hardness and lap shear test, were also evaluated.

Experimental procedure

The chemical compositions of bonded materials are listed in Table 1. The thickness of 6061-T6 was 2 mm, while 5052-H112 was 1 mm in thickness. To make a lap joint, the bottom of the tool must extend through the bottom of the top sheet and into the bottom sheet, creating a metallurgical bond between the two sheets. Schematic drawings of the lap joint process and lap shear test specimens are shown in Fig. 1. For examination of various microstructural features with joint constructions, FSW process in the present study is divided into cases A and B. Case A represents the friction stir lap welding construction of the fixture of 6061 Al located on top sheet at the retreating side and 5052 Al on the bottom sheet at the advancing side. Case B represents the friction stir lap welding construction of 5052 Al located on top sheet at the retreating side and 6061 on the bottom sheet at the advancing side.

Table 1 Chemical compositions of the base metals

	Si	Mg	Mn	Fe	Cu	Cr	Ti	Zn	Al
6061	0.691	1.131	0.113	0.299	0.212	0.154	0.011	0.011	Rest
5052	0.053	2.652	0.008	0.127	0.002	0.182	–	0.006	Rest

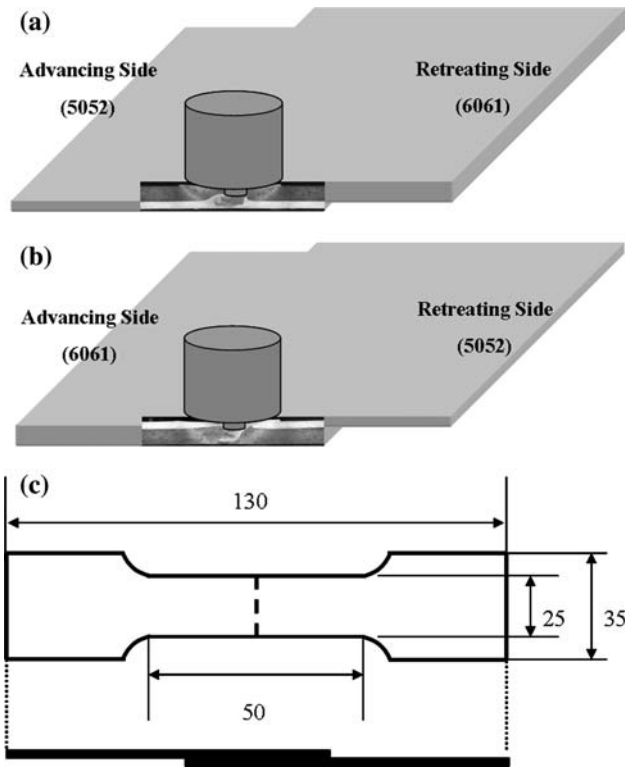

Fig. 1 Schematic illustration of friction stir welding process representing lap joint constructions: case A (**a**) and case B (**b**), and overlap shear test specimens (**c**)

Among the FSW parameters, tool rotation speed and welding speed were considered in the present study. Tool rotation speed was varied from 1,250 to 3,600 rpm at the fixed welding speed of 267 mm/min, while welding speed was varied from 127 to 507 mm/min at the fixed 1,600 rpm tool rotation speed. Welding tool was rotated clockwise and was tilted by 3° to provide compressive force to the stirred weld zone.

Microstructures of the weld zone were examined using Optical Microscopy (OM) and Transmission Electron Microscopy (TEM). The optical microstructures near the weld zone were observed by the conventionally polished and etched specimens. To inspect microstructures in the weld zone by TEM, FSW zone of similar 5052-H112 with 4-mm thickness was practically observed by TEM and that of similar 6061-T6 was referenced by our previous results [8] because the individual grain structure in the dissimilar lap weld zone cannot be clearly distinguished by TEM. For TEM observation, thin-foil disk specimens with 3-mm diameter were cut from the base metal and stir zone using an EDM (electron discharge machine), and mechanically polished to be 30 μm thickness. Transparent hole was produced by twin-jet electro polishing in nitric acid/methanol solution at 243 K. These thin foils were observed using a JEOL TEM at 300 kV. The composition of the second particles was analyzed by Energy Dispersive Spectroscopy (EDS) equipped in TEM.

The Vickers hardness profile of the weld zone was measured on a cross section perpendicular to the welding direction with a 100 gf load for 10 s. The mid-lines of both top and the bottom sheets were tested throughout the cross section.

The strength of the lap joints loaded nominally in lap shear was evaluated. In an ideal lap shear test (no bending and no sheet interface present), the tensile stress in the top and bottom sheets progressively decreases from a maximum at the loaded end to zero at the unloaded end. In a real shear test, particularly *if no guides are used*, additional tensile stresses will be generated at the bottom of the loaded side of the top sheet and at the top of the loaded side of the bottom sheet. Corresponding compression stress components will be generated on the opposite side of the sheets. These stresses arise due to bending of the sheets around the axes perpendicular to the loading direction and passing through points near the edges of the metallic-bonded interface. These bending stresses increase the severity of the test and may be deleterious when the lap joint interface has components normal to the nominal shear-loading direction [6]. Considering this test severity, all lap shear tests were performed using Instron machine with 5,000 kgf maximum load at a constant crosshead

displacement rate of 1 mm/min. The maximum fracture load and fractured location were recorded for each specimen. In this study, 5052 parts were gripped at the loading part regardless of cases A and B.

Results and discussion

Figure 2 shows the representative surface images of lap joints between 6061 and 5052 Al alloy in case A (a, b) and case B (c, d) with a condition of 1,600 rpm and 267 mm/min. Surface appearances from the other welding conditions were similar, but with slight differences in the amount of released burr and the area of weld. The surface morphologies are very smooth in both upper (crown) and bottom surfaces, where no porosity and defect line are observed. However, more irregular weld line on upper surface is observed in case B (c) than case A (a) because a thinner 5052 Al alloy has less resistance to plastic deformation when it is directly contacted with the rotating tool shoulder.

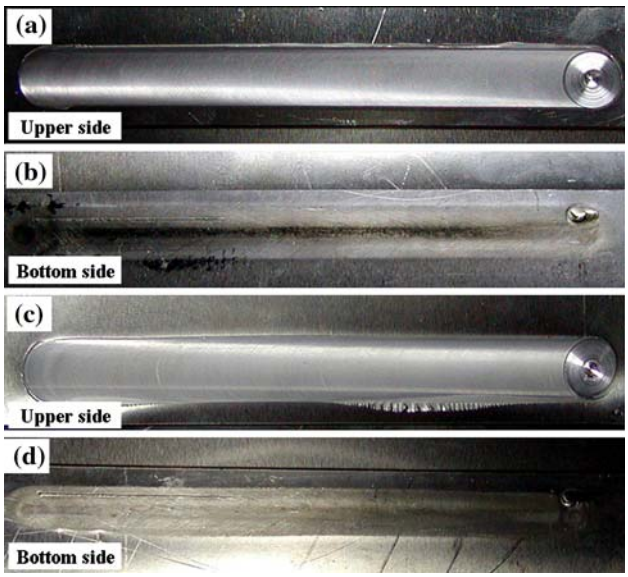

Fig. 2 Surface images of lap joints between 6061 and 5052 Al alloys in case A (**a**, **b**) and case B (**c**, **d**) with the condition of 1,600 rpm and 267 mm/min

Figure 3 shows the optical macrostructures of the weld zone with various welding conditions eonehpen welding speed and welding speed was changed from in case A. Figure 3a–c represents the weld zones with tool rotation speed, while Fig. 3d–f represents the weld zones with welding speed. No weld zone defect regardless of welding conditions means that the lap joints between 6061 and 5052 were successfully achieved under case A condition. Overall, the area of the weld zone (weld nugget) increases with increasing tool rotation speed, while the welding speed does not clearly affect the area of the weld zone. The area of the weld zone significantly depended on the heat generation during FSW. The higher tool rotation speed and lower welding speed have been known for generation of higher heat input [9, 10].

Complex metal flows such as intercalation (lamellar) structure between two materials and the onion ring structure are clearly observed. Material flows (vertical transport of materials), i.e., downward tendency of 6061 from top sheet and upward tendency of 5052 from bottom sheet, were characterized in case A. Vertical transport increased and both 6061 and 5052 were more deeply penetrated into each other with increasing tool rotation and decreasing welding speed. At lower tool rotation speed and higher welding speed, vertical transportation of 5052 Al alloy does not reach the mid-plane of the weld; however, at higher tool rotation speed and lower welding speed, 5052 Al alloy extends to more than two-third of the weld height. The onion ring pattern at 3600 rpm and 267 mm/min

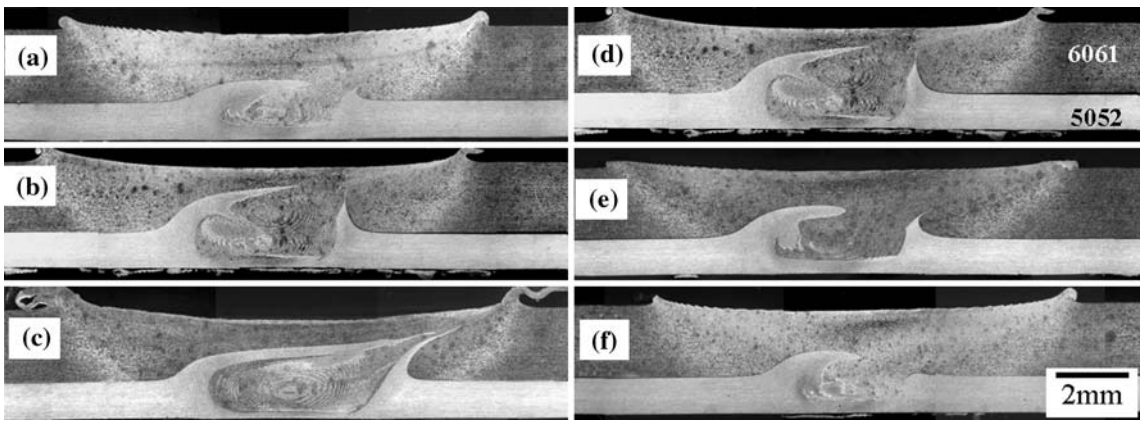

Fig. 3 Optical macroimages of lap-jointed 6061 and 5052 in case A with various welding conditions: (**a**) 1250 rpm, (**b**) 2,500 rpm, and (**c**) 3600 rpm at fixed 267 mm/min, while (**d**) 127 mm/min, (**e**) 267 mm/min, and (**f**) 507 mm/min at fixed 1,600 rpm

welding condition shows a complete form without disconnection.

Figure 4 shows the optical macrostructures of the weld zone eonehpen welding speed and welding speed was changed from in case B with various welding conditions. Figure 4a–c represents the weld zones with tool rotation speed, while Fig. 4d–f shows the weld zones with welding speed. Similarly, the weld zones were composed of the intercalating structure and complex metal flow. Especially, the downward tendency of 5052 Al into 6061 on bottom sheet is dominant. Onion ring pattern is clearly observed in overall weld nugget at higher tool rotation speed and lower weld speed; however, under other welding conditions, onion ring pattern was not complete. Onion ring pattern was formed only in the retreating part at lower tool rotation speed and higher welding speed, and then represented a complete ring pattern at higher tool rotation speed and lower welding speed.

Characterizations of FSW lap joint weld zone with various welding conditions are summarized by some interesting features. In case A, thinner 5052 Al alloy on bottom sheet was pulled-up into the 6061 side in both retreating side and advancing side, especially in advancing side. Part of 5052 Al alloy below the tool pin moved downward and thickness of 5052 Al alloys in the weld zone resultantly decreased. With increasing tool rotation speed and decreasing welding speed, pull-up of 5052 Al increased in advancing and retreating side and pulled-up two sides of 5052 Al alloy were connected at the upper retreating side of 6061 Al alloy. Onion ring patterns were completely formed and thickness of 5052 Al remarkably decreased due to pull-up. Reversely, in case B, pull-down of thinner 5052 Al alloy on top sheet was observed especially in retreating side. Interface between 5052 and 6061 was slightly upward from initial joint line. With increasing tool rotation speed and decreasing welding speed, onion ring pattern was gradually completed.

Figure 5 shows the optical microstructures of the weld zone in case A with the welding condition of 1,600 rpm and 267 mm/min. The grain size (a) of the 5052 Al in the SZ is finer than that (b) of the 6061 Al alloy, while both of them represent equaxed recrystallized grains. From the different grain size and etching response of two materials, individual grains can be distinguished between 6061 Al and 5052 Al alloys in complex mixed structure in the SZ. Onion ring pattern characterized by the stack of two materials is observed; however, the formation of ring pattern is not completed as shown in (c). Interfaces between dissimilar materials were also created and represented the mixing of two materials (d and f) and non-straight line (e). Reaction layer and second phase were not identified at the interface because the temperature and maintaining time were not sufficient for the diffusion due to the solid-state bonding of FSW.

Figure 6 shows the optical microstructure of the weld zone in case A with the tool rotation speed of 3,600 rpm and welding speed of 267 mm/min. Many scratch-like lines are observed in the weld zone but identified as interfaces. The onion ring patterns are more repeatedly observed and are mainly composed of 6061 Al alloys.

Figures 7 and 8 show the optical microstructures in case B with tool rotation speed of 1,600 rpm and 3,600 rpm at the fixed welding speed of 267 mm/min, respectively. In Fig. 7, equaxied and fine grain structures (b, d, and e) are also characterized in the SZ of 5052 and 6061 Al alloys. Especially, part of the onion ring stack is mainly composed of 5052 which was fixed at the retreating side. As the tool rotation speed increased, as shown in Fig. 8, the microstructures of the weld zone represent more complex features and large part of the onion ring was 5052 Al alloy.

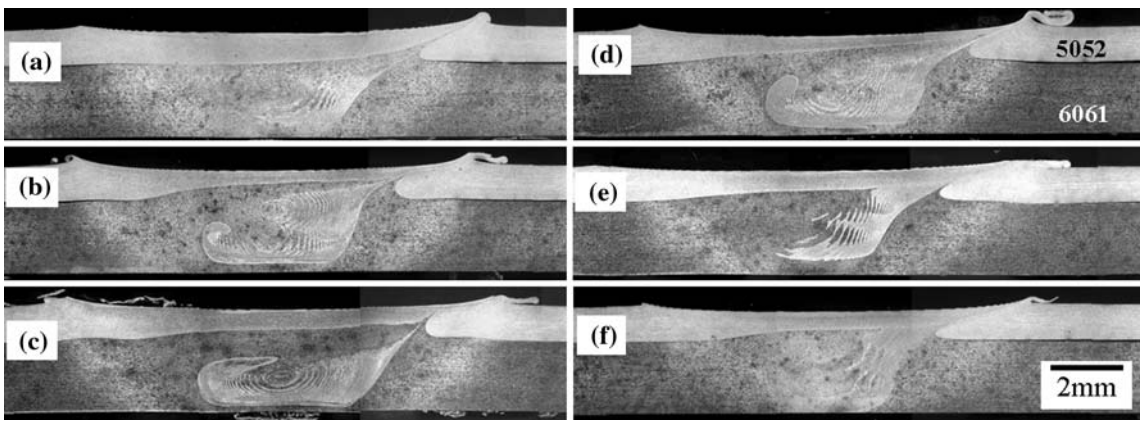

Fig. 4 Optical macroimages of lap-jointed 6061 and 5052 in case B with various welding conditions: (**a**) 1250 rpm, (**b**) 2,500 rpm, and (**c**) 3600 rpm at fixed 267 mm/min, while (**d**) 127 mm/min, (**e**) 267 mm/min, and (**f**) 507 mm/min at fixed 1,600 rpm

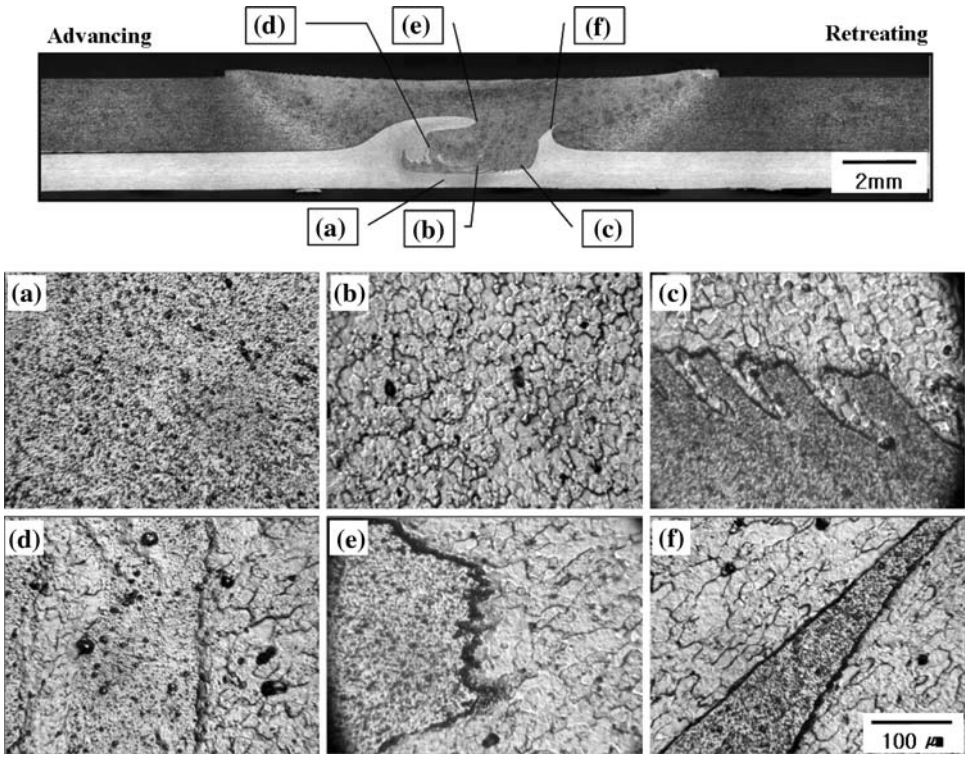

Fig. 5 Optical microstructures of the weld zone in case A with the welding condition of 1,600 rpm and 267 mm/min: (**a–f**) representing each region of the weld zone marked in macroimages

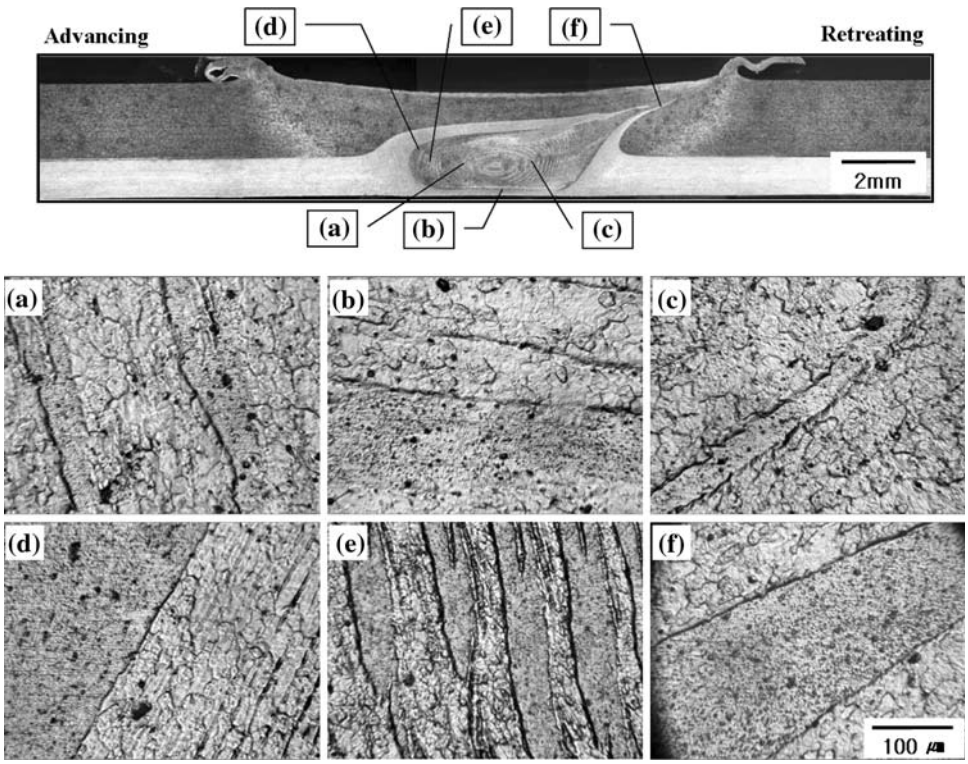

Fig. 6 Optical microstructures of the weld zone in case A with the welding condition of 3,600 rpm and 267 mm/min: (**a–f**) representing each region of the weld zone marked in macroimages

Figure 9 shows the hardness distributions near the weld zone in the middle of both the top and the bottom sheets in case A with various welding conditions. Figure 9a and b represents the hardness distribution in the middle of 6061 Al plate on the top sheet with various tool rotation speeds and welding speeds, respectively. Hardness of 6061 base metal shows a range of 100–110 HV, while the weld zone shows a softening region which spreads 10 mm from the

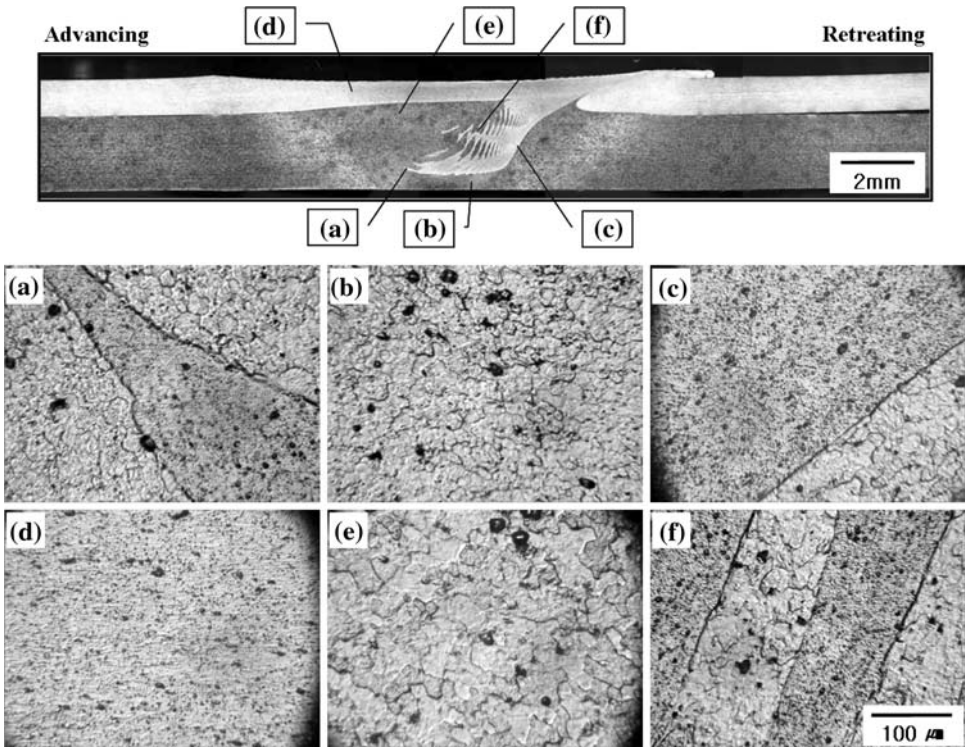

Fig. 7 Optical microstructures of the weld zone in case B with the welding condition of 1,600 rpm and 267 mm/min: (**a**–**f**) representing each region of the weld zone marked in macroimages

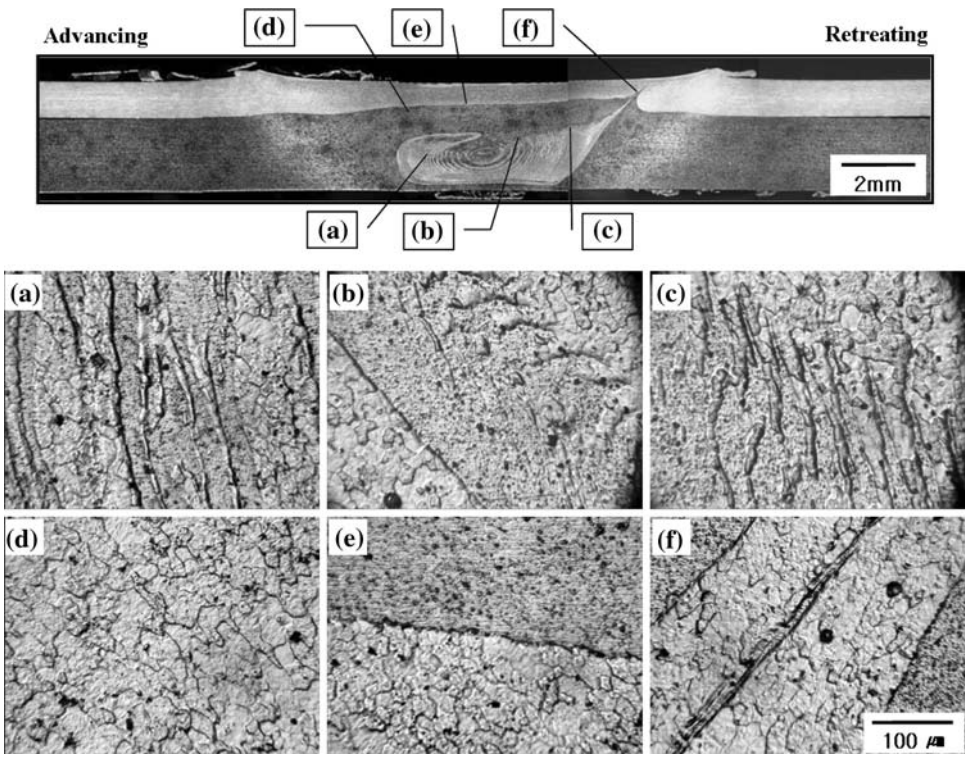

Fig. 8 Optical microstructures of the weld zone in case B with the welding condition of 3,600 rpm and 267 mm/min: (**a**–**f**) representing each region of the weld zone marked in macroimages

weld center regardless of the advancing and retreating side. The central weld zone including 5-mm region from the center shows a slightly higher value, 75 HV, than that (65 HV) of a lower hardness region which was located 10 mm away from the weld center. These are similar results of hardness distribution of FSWed 6XXX series weld zone from reported papers [11–14]. Lee et al. reported that SZ and HAZ of 6061-T6 were characterized by dissolution or re-precipitation and coarsening of precipitates, respectively [8], which were responsible for a lower

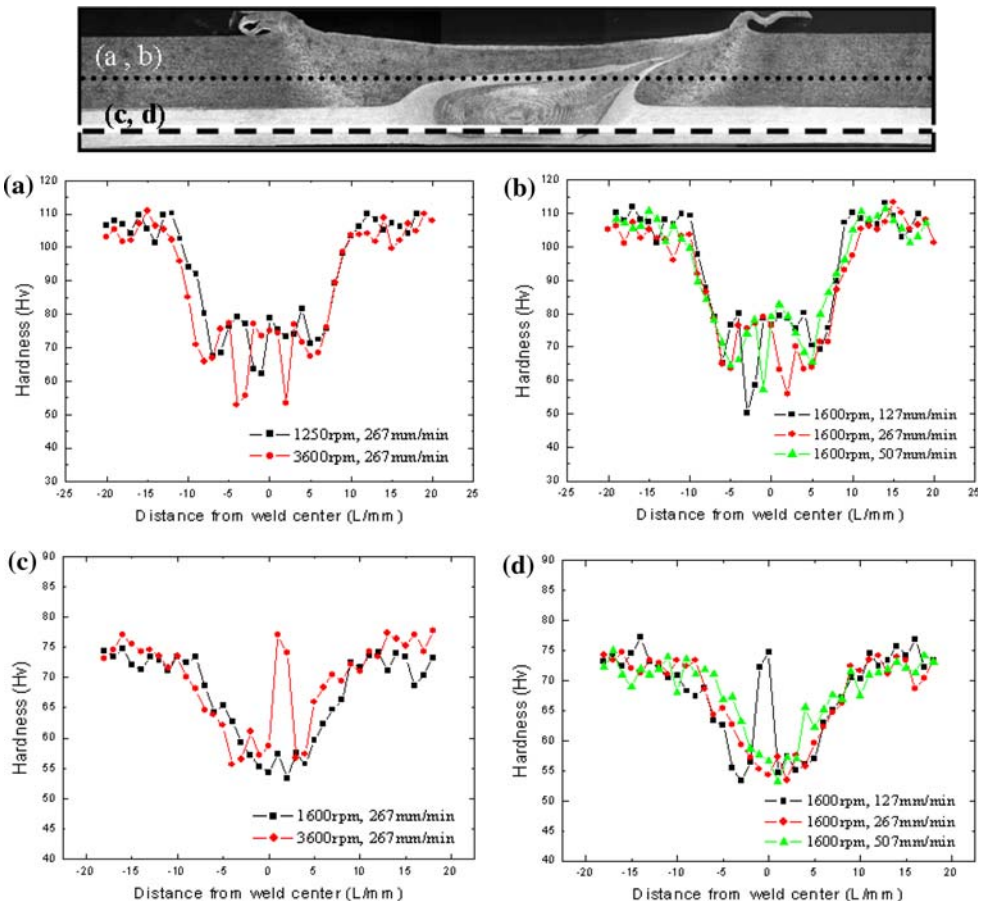

Fig. 9 Hardness distribution near the weld zone in the mid-lines of the both the top and the bottom sheet in case A with various welding conditions: (**a**) and (**b**) measuring on top sheet of 6061 Al alloy, (**c**) and (**d**) measuring on the bottom sheet of 5052 Al alloy

hardness. However, because SZ had fine grains with higher angle grain boundary and higher density of dislocation, hardness of the SZ was slightly higher than that of HAZ.

However, remarkably lower hardness (range from 50 to 60 HV) was measured in some parts of the SZ and measured spots with lower hardness than 60 HV increased with increasing tool rotation speed and decreasing welding speed. The minimum hardness region in the SZ should be related to the recrystallized grains of 5052 Al alloy. Figure 9c and d represents hardness distribution in the middle of 5052 Al plate on bottom sheet with tool rotation speed and welding speed, respectively. Hardness of 5052 Al alloy represents 75 HV of the average value, and also shows the softening region which reaches 7 mm from the weld center. Minimum hardness of the weld zone is 55 HV. Similarly, higher hardness was measured in some regions of the SZ at conditions of higher tool rotation speed and lower welding speed. This is related to the 6061 Al alloy which was transported from top sheet because the hardness value is consistent with that of SZ of top sheet.

Figure 10 shows the TEM microstructures of similar 5052 Al-H112 with 4-mm thickness with each region (BM (a), SZ (b)), and hardness distribution (c) near the weld zone. Hardness of the weld zone shows a similar or slightly higher value than that of base metal. TEM microstructure reveals that a slightly higher hardness of the weld zone is attributed to the fine grain size, higher dislocation density, and second particle (Al_3Fe). These structures might be introduced by severe plastic deformation and accompanying frictional heat. From the results of FSWed solid solution-hardened Al alloy [15, 16], hardness of the weld zone was similar or higher than that of the base metal through the weld zone. However, hardness distribution near the weld zone in 5052 part showed lower hardness than that of the 5052 BM. 5052 Al alloy fixed on bottom sheet cannot be mostly affected by the plastic deformation of weld tool, but only received the pull-down force of rotation pin. Therefore, the weld zone of 5052 Al in case A might be affected by frictional heat. Thermal annealing effect was mainly induced in 5052 Al weld zone. From this reason, the weld zone of 5052 Al alloy represented a lower value than that of the base metal.

Table 2 and Fig. 11 show the lap shear test results and fractured specimens with welding conditions, respectively. Totally, fracture loads are higher in case A than those in case B. In case A, fracture locations were not constant with welding conditions; however in case B, fracture always occurred at 5052 Al fixed on top sheet in retreating side.

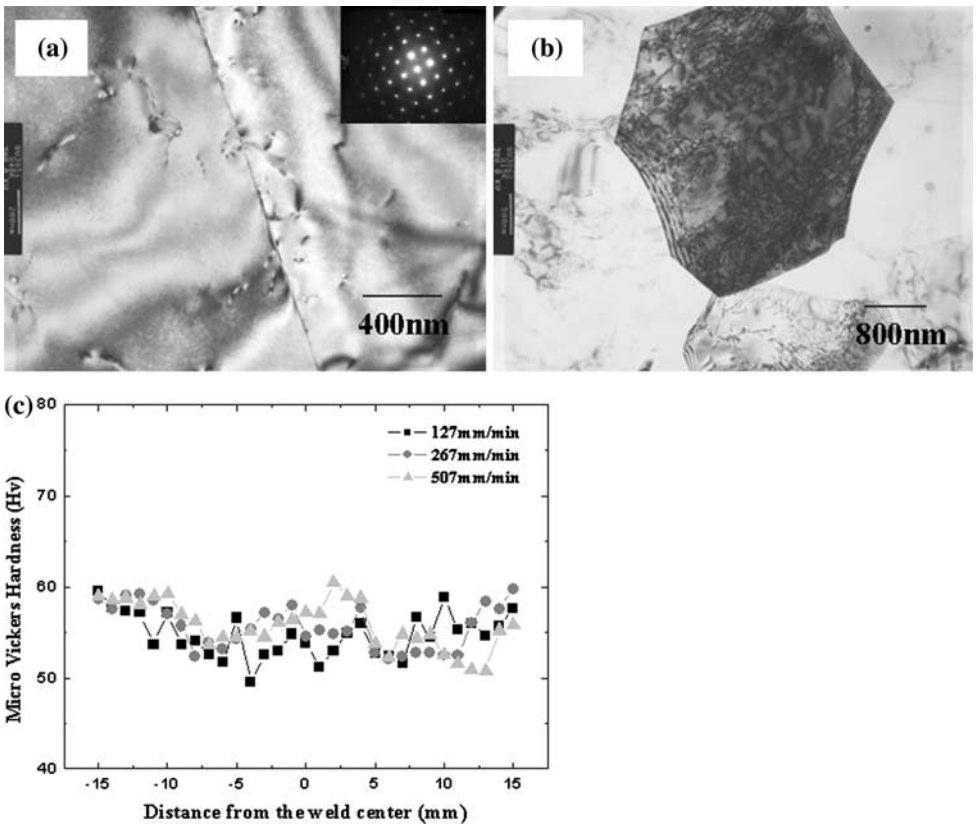

Fig. 10 TEM microstructures of the base metal (**a**), the stir zone (**b**), and hardness distribution near the weld zone (**c**) in similar 5052 FSW joints

Table 2 Overlap shear test results with various welding conditions

Case A	F load (kN)	F location	Case B	F load (kN)	F location
1250/267	5.6	B.A.5052	1250/267	2.7	T.R.5052
2500/267	2.2	T.R.6061	2500/267	2.2	T.R.5052
1600/127	4.2	T.R.6061	1600/127	1.5	T.R.5052
1600/507	6.0	B.A.5052	1600/507	2.6	T.R.5052

F: Fracture, T: Transition, R: Retreating, B: Base metal, A: Advancing

Through-nugget fracture was not observed under applied welding conditions in present study. Higher fracture load of 6.0 kN was acquired at lower tool rotation speed and higher welding speed in case A. In case B, despite a lower facture load being measured, similar results depending on welding conditions were observed. Weak bonds were obtained under the welding conditions of higher tool rotation speed and lower welding speed, which resulted in as much interface pull-up as possible and more introduction of unbonded interface into the weld zone. As shown in Fig. 11a, fractures occurred at transition region of 6061 top sheet, which means that the unbonded region might be acted as the crack initiation site during test and responsible for lower tensile load. Because higher welding and lower tool rotation speed resulted in fewer pull-ups, the maintenance of thickness of bottom sheet of 5052 Al alloy, and less introduction of unbonded region into the weld zone, higher fracture load was

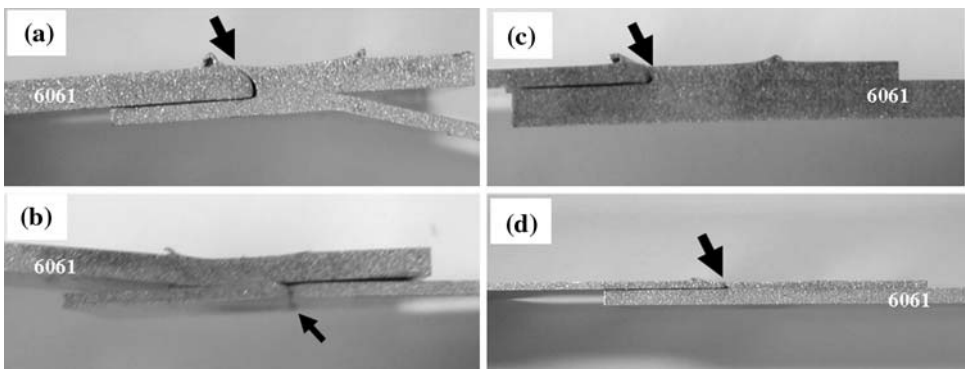

Fig. 11 Fractured specimens after lap shear test with various welding conditions: (**a**) 2,500 rpm, 267 mm/min and (**b**) 1,600 rpm, 507 mm/min: case A, (**c**) 2,500 rpm, 267 mm/min and (**d**) 1600 rpm, 507 mm/min: case B

acquired and fracture occurred in a region away from the weld zone as shown in Fig. 11b. Excessive vertical movements of materials can badly affect the joint strength, which means less pull-up (less introduction of unbonded region into the weld zone) gives higher bond strength.

Effect of other factors such as thickness difference, load direction, and specimen geometry of shear test, must also be deeply analyzed and these remain as future works.

Conclusion

Lap joint FSW between 6061 and 5052 Al alloys with different thickness was carried out under various welding parameters. Main conclusions are as followed:

1. Interface morphologies were characterized by interface pull-up (case A) and pull-down (case B) in the advancing and retreating side; however, at central weld zone, interface was inversely pulled-down (case A) and pulled-up (case B), respectively. Due to vertical movement of mixed materials, thickness of thinner 5052 Al resultantly lessened.
2. As the tool rotation speed increased and welding speed decreased: (1) pull-up and pull-down at retreating and advancing side (introduction of unbonded region) increased, (2) thickness of thinner 5052 Al alloy gradually lessened, and (3) onion ring patterns were completed without disconnection and lightly observed in overall weld zone.
3. Fracture load was lower at higher tool rotation speed and lower welding speed, because increased pull-up and pull-down made the interfaces more sharp and introduction of unbonded region into the weld zone, which resulted in stress concentration. The lessened thickness of 5052 Al alloy also contributed to lower fracture load.
4. Hardness of the weld zone shows a lower hardness than those of 6061 Al and 5052 Al base metals due to the loss of precipitates and annealing effect, respectively, in case A. Due to metal flow to each other, hardness in the weld zone maintained individual hardness depending on measuring points.
5. Joint strengths of FSWed lap joints mainly depended on the interface morphology and vertical transport of each material with welding conditions.

References

1. Thomas WM et al (1995) Friction stir butt welding. United States Patent #5,460,317
2. Johnsen MR (1999) Weld J 78:35
3. Okamura H, Aota K, Ezumi M (2000) J Jpn Inst Light Met 50:166
4. Murr LE, Liu G, McClure JC (1997) J Mater Sci Lett 16:1801
5. Mishra RS, Ma ZY (2005) Mater Sci Eng R 50:1
6. Cederqvist L, Leynolds AP (2001) Weld J Res Suppl 80:281
7. Cederqvist L, Leynolds AP (2000) In: Proceeding of the 2nd international symposium on friction stir welding, Gothenburg, Sweden
8. Lee WB, Yeon YM, Jung SB (2004) Mater Trans (JIM) 45:1700
9. Chen CM, Kovacevic R (2003) Int J Mach Tool Manu 43:1319
10. Ulysse P (2002) Int J Mach Tool Manu 42:1549
11. Liu G, Murr LE, Niou CS et al (1997) Scripta Mater 37:355
12. Murr LE, Liu G, McClure JC (1998) J Mater Sci 33:1243
13. Sato YS, Kokawa H, Enomoto M et al (1999) Metall Mater Trans A 30:2429
14. Sato YS, Urata M, Kokawa H (2002) Metall Mater Trans A 33:625
15. Svensson LE, Karlsson L, Larsson H et al (2000) Sci Technol Weld Joining 5:285
16. Sato YS, Park SHC, Kokawa H (2001) Metall Mater Trans A 32:3033